INTERNATIONAL JOURNAL FOR NUMERICAL METHODS IN FLUIDS, VOL. 9, 1195–1206 (1989)

A BOUNDARY ELEMENT METHOD FOR A NON-LINEAR FREE SURFACE PROBLEM

E. CAMPANA, F. LALLI AND U. BULGARELLI
INSEAN–Italian Ship Model Basin, Via di Vallerano 139, I-00128 Rome, Italy

SUMMARY

In this paper a numerical method to compute the wave resistance of a body submerged in a free stream of finite and infinite depth is presented. Non-linear effects on the free surface are taken into account by an iterative procedure; the solution is in the form of a single-layer potential. For the 2D problem, results are shown for both the cases of finite and infinite depth of the fluid domain, with special emphasis on the supercritical flow in which the consistency of the scheme is pointed out. The method is also extended to the 3D case of a spheroid submerged in deep water. All the results presented are compared with experimental data and analytical solutions available in the literature.

KEY WORDS Free boundary problem Potential flow Wave resistance BEM

1. INTRODUCTION

In the present work the wave resistance problem is studied from a numerical point of view. A simple shaped body submerged in a free stream of finite and infinite depth is considered. The perturbation of the free surface (due to the presence of the body) and the pressure field around the body itself are computed, the potential flow being solved by means of the boundary element method. This is a basic problem of great practical importance in naval engineering: the optimum ship hull, from the resistance point of view, is the one producing the smallest amplitude waves.[1] Many theoretical studies on the ship wave resistance problem are available in the literature.[2–7] Experimental methods have also been proposed.[8,9] A systematic presentation and a complete bibliography are given in References 1 and 10.

In recent years, several researchers have been studying ship waves by means of numerical methods that allow one to solve the problem by taking into account the non-linear behaviour of the free surface, which is neglected in the analytical and experimental methods mentioned above. Dawson[11] proposed a simple numerical method, based on the linearized free surface conditions, which is useful for practical applications to low-Froude-number ship motions. However, as the Froude number grows, the non-linear effects become more and more important. For this reason, there has been a rapid development in non-linear numerical methods.[12,13]

In the present work the ideas expressed in Reference 12 are followed, but we use an implicit numerical scheme for the non-linear terms and different assumptions in deriving the non-linear free surface boundary conditions by means of a Taylor series. Some numerical results for two- and three-dimensional simple shaped submerged bodies have been obtained. The non-linear method is compared with the linear one and with the experimental data taken from Reference 12 for the 2D

0271–2091/89/101195–12$06.00

Received August 1988
Revised May 1989

case of an elliptical cylinder submerged in deep water. This last body has also been considered in a finite depth domain (see Reference 14 for existence and uniqueness of the solution) in both the cases of subcritical and supercritical flow. The capability of the proposed numerical procedure to follow the peculiar behaviour of the physical phenomenon is shown in comparison with the experimental data available in Reference 15. Finally, in the 3D case the solution obtained has been compared with the analytical solution given in Reference 16.

2. THE MATHEMATICAL MODEL

We consider the irrotational steady state flow of an incompressible fluid past a submerged body. The fluid domain is bounded above by a free surface and unbounded in the other directions. The velocity scalar potential satisfies Laplace's equation inside the fluid field:

$$\nabla^2\Phi(x, y, z)=0, \quad x, y, \Phi_z \in \mathbb{R}^3 \setminus \bar{B} \cap \{z: -\infty < z < \zeta(x, y)\}, \tag{1}$$

where $\bar{B}=B \cup \partial B \subset \mathbb{R}^3$ is the body and $\zeta(x, y)$ expresses the free surface which will be denoted by S. Equation (1) is associated to the following boundary conditions:

$$\Phi_x\zeta_x+\Phi_y\zeta_y-\Phi_z=0 \qquad \text{on } S, \tag{2}$$

$$\zeta=-(1/2g)(\Phi_x^2+\Phi_y^2+\Phi_z^2-U_\infty^2) \qquad \text{on } S, \tag{3}$$

$$\Phi_n=0 \qquad \text{on } \partial B, \tag{4}$$

$$\lim_{x\to-\infty} \nabla\Phi=U_\infty. \tag{5}$$

In the case of finite depth, the following boundary condition has to be imposed at the bottom:

$$\Phi_n=0. \tag{6}$$

The solution of the problem (1)–(5) is computed by means of a numerical method based on an integral formulation that implies a second-type Fredholm equation.

The potential Φ is expressed as the sum of three terms:

$$\Phi=U_\infty x+\varphi+\tilde{\varphi}, \tag{7}$$

where the first term is the undisturbed flow potential, the second term is the double model potential which takes into account the interaction among the free stream, the body and its image, and the third term is the perturbation potential due to the presence of the free surface as well as its coupling with the body. If the bottom is considered, an additional term must obviously be included.

3. THE FREE SURFACE BOUNDARY CONDITIONS

The problem (1)–(5) is non-linear because of the presence of quadratic terms in the free surface conditions (2) and (3) and also because these conditions are to be applied on the unknown surface S. A great simplification is introduced by considering the Taylor series expansion around the plane $z=0$ (undisturbed free surface) of conditions (2) and (3). We obtain an approximation scheme that assumes the flow to be a small perturbation of an undisturbed free surface flow and the shape of the free surface itself to be sufficiently smooth. Hereafter, in order to avoid cumbersome notation, only the 2D case is described:

$$[\zeta_x(1+\varphi_x+\tilde{\varphi}_x)-\tilde{\varphi}_z]_{z=0}+\frac{\partial}{\partial z}[\zeta_x(1+\varphi_x+\tilde{\varphi}_x)-\tilde{\varphi}_z]_{z=0}\,\zeta=O(\zeta^2), \tag{8}$$

$$\zeta = -\frac{Fr^2}{2}[2(\varphi_x + \tilde{\varphi}_x) + (\varphi_x + \tilde{\varphi}_x)^2 + \tilde{\varphi}_z^2]_{z=0} - \frac{Fr^2}{2}\frac{\partial}{\partial z}[2(\varphi_x + \tilde{\varphi}_x) + (\varphi_x + \tilde{\varphi}_x)^2 + \tilde{\varphi}_z^2]_{z=0}\zeta + O(\zeta^2), \tag{9}$$

where $Fr = U_\infty/\sqrt{(gL)}$ is the Froude number and L is the body length.

Using (8) and (9), the following free surface boundary conditions are deduced in the linear case:

$$\zeta_x(1 + \varphi_x) - \tilde{\varphi}_z = 0, \tag{10}$$

$$\zeta = -(Fr^2/2)[2(\varphi_x + \tilde{\varphi}_x) + \varphi_x^2 + 2\varphi_x\tilde{\varphi}_x]; \tag{11}$$

and in the non-linear case

$$\zeta_x(1 + \varphi_x + \tilde{\varphi}_x) - \tilde{\varphi}_z - \zeta\tilde{\varphi}_{zz} = 0, \tag{12}$$

$$\zeta = -(Fr^2/2)[2(\varphi_x + \tilde{\varphi}_x) + (\varphi_x + \tilde{\varphi}_x)^2 + \tilde{\varphi}_z^2]. \tag{13}$$

4. THE NUMERICAL MODEL

In the discrete problem the surface of the body ∂B and a local portion of the undisturbed free surface S are discretized with linear elements; the total numbers of body and free surface panels are respectively BE and SE. A discrete distribution of piecewise-constant simple sources extending over these surfaces, with surface densities σ, $\Delta\sigma$ and $\tilde{\sigma}$, generates the simple layer potentials

$$\varphi_i = \sum_{j=1}^{\mathrm{BE}} \sigma_j \int_{l_j} k_{ij}\,\mathrm{d}l_j, \tag{14}$$

$$\tilde{\varphi}_i = \sum_{j=1}^{\mathrm{BE}} \Delta\sigma_j \int_{l_j} k_{ij}\,\mathrm{d}l_j + \sum_{j=1}^{\mathrm{SE}} \tilde{\sigma}_j \int_{l_j} g_{ij}\,\mathrm{d}l_j \tag{15}$$

in which

$$k_{ij} = \log|p_i - q_{\mathrm{B}_j}| + \log|p_i - q^*_{\mathrm{B}_j}|, \qquad g_{ij} = \log|p_i - q_{S_j}|,$$

where p is a field point, q ($\in\partial B$ or S) is a source point and $q^*_B(\in\partial B^*)$ is a source point, with ∂B^* the image of ∂B above the undisturbed free surface. In the 3D computation $|p-q|^{-1}$ is used instead of the logarithmic kernel.

In order to initialize the iterative procedure, we first need to compute the double model source strength using condition (4) (once this problem is solved, the value of φ is known definitively):

$$(1 + \varphi_{x_i})\cos\widehat{xn_i} + \varphi_{z_i}\cos\widehat{zn_i} = 0, \quad i \in \mathrm{BE}. \tag{16}$$

Then the perturbation potential source strength can be computed using linear conditions (10) and (11):

$$\begin{aligned} \tilde{\varphi}_{x_i}\cos\widehat{xn_i} + \tilde{\varphi}_{z_i}\cos\widehat{zn_i} &= 0, && i \in \mathrm{BE}, \\ (1 + \varphi_{x_i})\varphi_{xx_i}\tilde{\varphi}_{x_i} + (1 + \varphi_{x_i})^2\tilde{\varphi}_{xx_i} + (1/Fr^2)\tilde{\varphi}_{z_i} &= -(1 + \varphi_{x_i})^2\varphi_{xx_i}, && i \in \mathrm{SE}, \end{aligned} \tag{17}$$

where

$$\tilde{\varphi}_{x_i} = \sum_{j=1}^{\mathrm{BE}} \Delta\sigma_j \int_{l_j} \frac{\partial k_{ij}}{\partial x_i}\,\mathrm{d}l_j + \sum_{j=1}^{\mathrm{SE}} \tilde{\sigma}_j \int_{l_j} \frac{\partial g_{ij}}{\partial x_i}\,\mathrm{d}l_j + \pi(\Delta\sigma_i + \tilde{\sigma}_i)\cos\widehat{xn_i}, \tag{18}$$

with analogous expressions for φ_x, $\tilde{\varphi}_z$ and φ_z. The linear wave elevation can be calculated next from (11).

The knowledge of the value of φ and of the linear approximations of $\tilde{\varphi}$ and ζ allows one to start the following iterative procedure:

$$
\begin{aligned}
&{}^{(K-1)}\zeta_{x_i}\,{}^{(K)}\tilde{\varphi}_{x_i} - {}^{(K)}\tilde{\varphi}_{z_i} + {}^{(K)}\tilde{\varphi}_{xx_i}\,{}^{(K-1)}\zeta_i = {}^{(K-1)}\zeta_{x_i}(1+\varphi_{x_i}) - {}^{(K-1)}\zeta_i\varphi_{xx_i},\\
&{}^{(K)}\tilde{\varphi}_{x_i}\cos\widehat{xn_i} + {}^{(K)}\tilde{\varphi}_{z_i}\cos\widehat{zn_i} = 0,
\end{aligned}
\tag{19}
$$

$$
{}^{(K)}\zeta_i = -(Fr^2/2)[2(\varphi_{x_i} + {}^{(K)}\tilde{\varphi}_{x_i}) + (\varphi_{x_i} + {}^{(K)}\tilde{\varphi}_{x_i})^2 + {}^{(K)}\tilde{\varphi}_{z_i}^2], \tag{20}
$$

until the difference between two successive locations of the free surface is sufficiently small. In order to avoid convergency problems, relaxation factors have been introduced in (19) and (20).

Finally, the wave resistance is computed by

$$
R_w = \tfrac{1}{2}\sum_{i=1}^{\mathrm{BE}} [2(\varphi_{x_i} + \tilde{\varphi}_{x_i}) + (\varphi_{x_i} + \tilde{\varphi}_{x_i})^2 + (\varphi_{z_i} + \tilde{\varphi}_{z_i})^2]\cos\widehat{xn_i}. \tag{21}
$$

We remark that the discretization of the second derivative appearing in (17) and (20) has been done by using a finite difference scheme; since the numerical solution depends strongly on the discretization used, numerical tests have been carried out to verify that the second-order four-point upwind operator, proposed in Reference 11, satisfies the asymptotical behaviour of a constant amplitude wave for the disturbance generated by a body in deep water. The proposed method has also been validated in the peculiar case of finite depth supercritical flow, in which the amplitude of the perturbation generated by the body should be rapidly damped.

5. NUMERICAL RESULTS

The numerical method has been used first to compute the wave pattern due to an elliptical cylinder moving with constant speed under the free surface at different Froude numbers. The numerical solutions computed by the linear and non-linear methods have been compared with a set of experimental data given in Reference 12.

Figure 1 shows the wave pattern as the Froude number increases. If this number is relatively small (case (a)), the three curves are almost coincident; when it is larger, the wave pattern computed by the non-linear method gives a better fit to the experimental data (case (b)). The last case shows the failure of both the numerical models at the highest Froude number, because they are not able to follow the onset of the breaking wave phenomenon.

Figures 2 and 3 show the computations made in order to check the capability of the proposed method when the bottom is considered. In Figure 2 the subcritical case is shown, where the amplitude of the downstream perturbation is constant. The pattern of a supercritical flow is described in Figure 3, where the perturbation is damped almost immediately, as expected. This behaviour is shown in Figure 4, which reproduces the experimental results from Reference 15.

Finally, the method has been applied in the Neumann–Kelvin formulation[17] to compute the wave pattern and the wave resistance for submerged spheroids.

In order to establish the minimum undisturbed free surface area that needs to be discretized and the minimum number of panels per wavelength, NPλ (assuming the wavelength to be $2\pi U_\infty^2/g$), a large number of numerical tests have been carried out. Figure 5 shows how the effect of a reduction in NPλ gradually influences the value of the wave resistance obtained. The same figure also shows how the computed wave resistance depends on the downstream extension of the free surface panelled region when NPλ is given (in this case NP$\lambda = 24$).

In Figure 6 the downstream perturbation behaviour is depicted for two bodies (sphere and prolate spheroid with eccentricity 0·9165) and for two values of the Froude number. In Figure 7 a

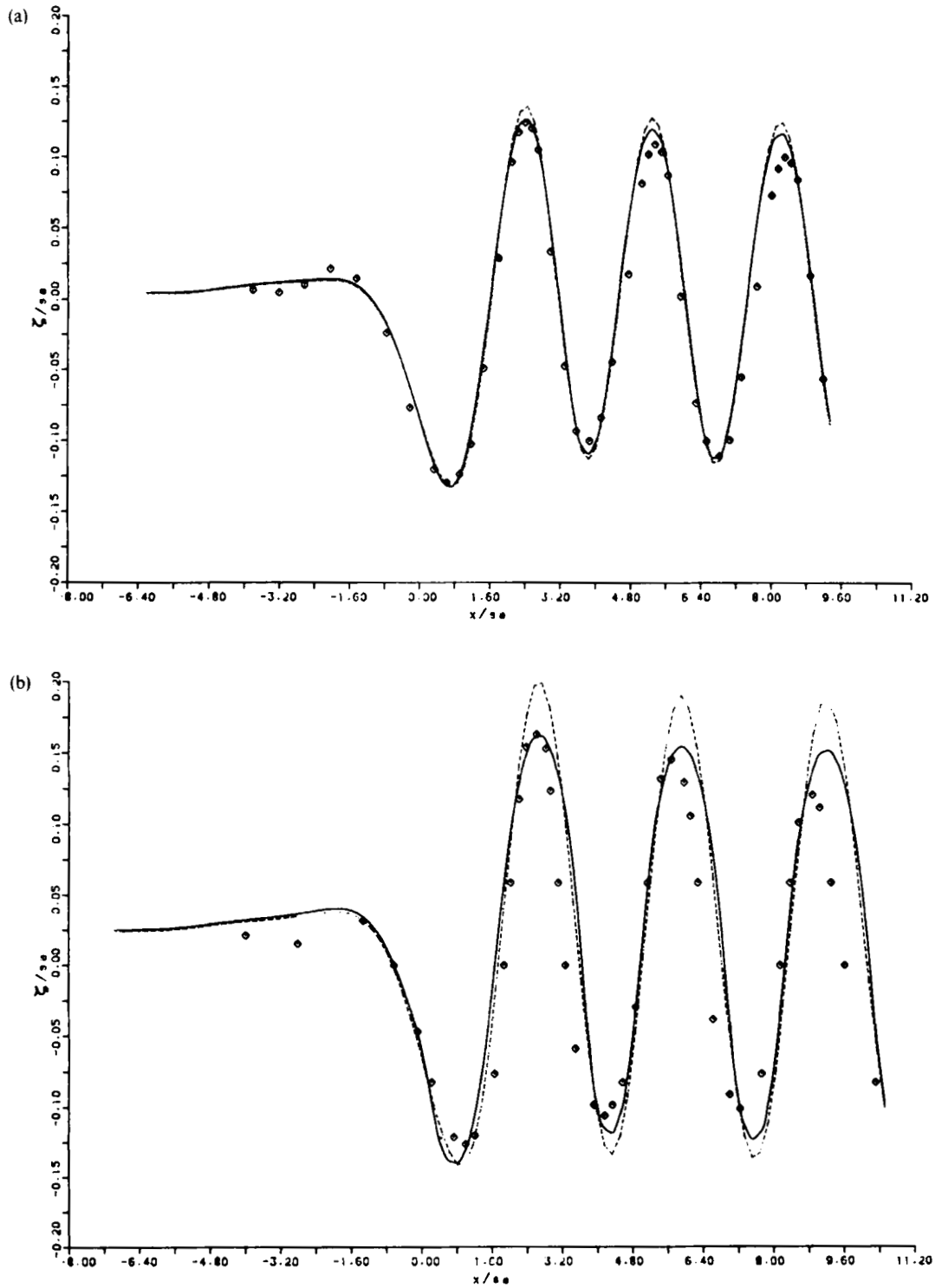
(a)
(b)
ζ/s₀
x/s₀
0.20
0.15
0.10
0.05
0.00
-0.05
-0.10
-0.15
-0.20
-8.00
-6.40
-4.80
-3.20
-1.60
0.00
1.60
3.20
4.80
6.40
8.00
9.60
11.20

Figure 1. (a, b)

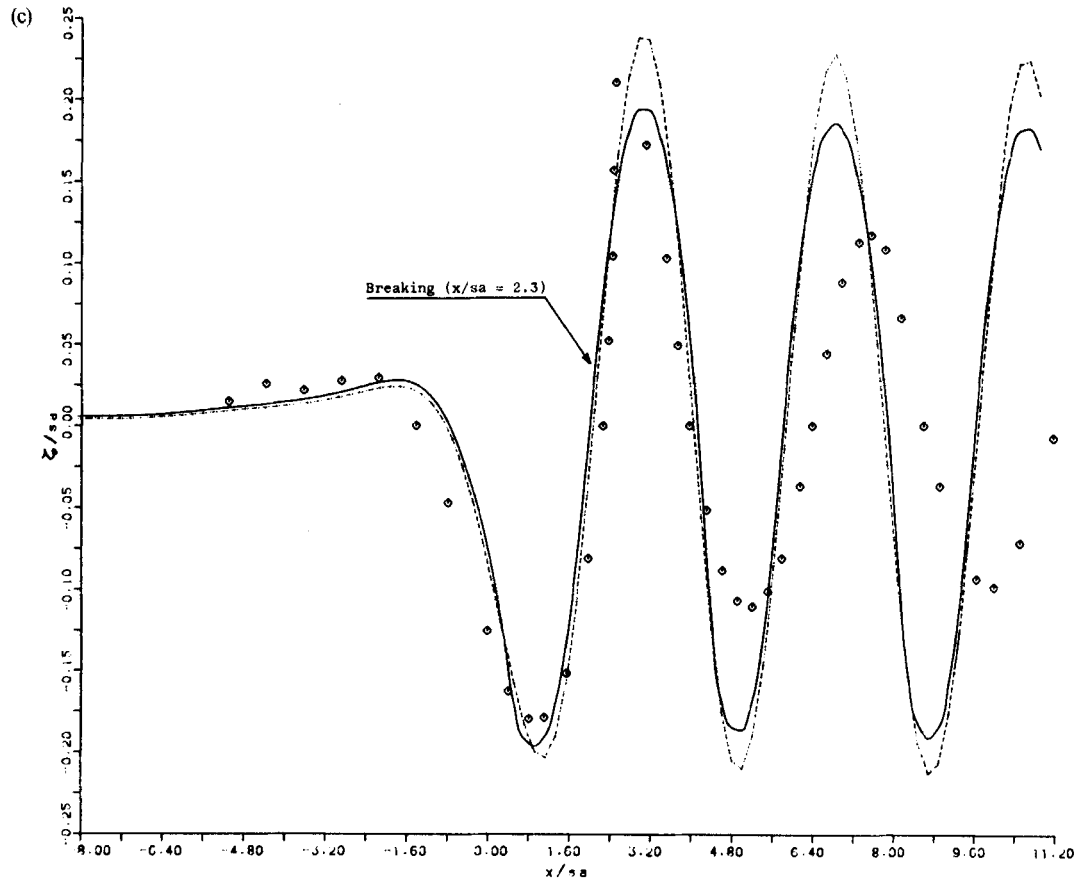

Figure 1. Two-dimensional wave pattern generated by a submerged elliptical cylinder in deep water; $sa/sb = 4$ (sa and sb are the major and minor semi-axes), $f/sa = 1{\cdot}7$ (f is the depth of the body centre). Froude number $Fr = U_\infty/\sqrt{(2 \times sa \times g)}$: (a) 0·50; (b) 0·53; (c) 0·57. Key: ○ ○ ○ ○ ○, experimental data;[12] – – – – – – – –, linear method; ————, non-linear method

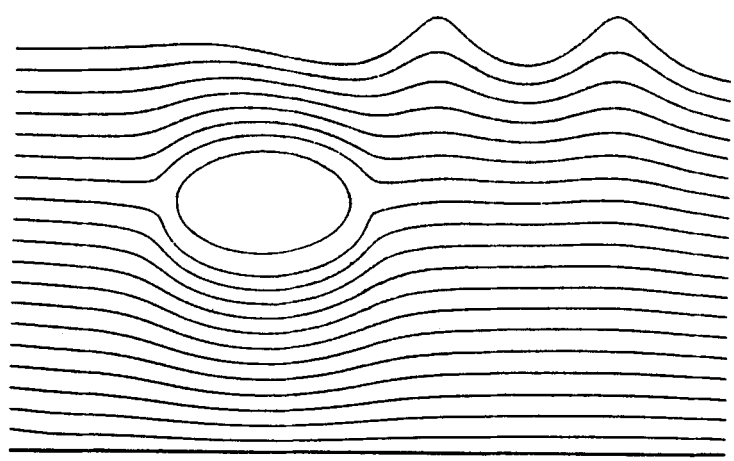

Figure 2. Numerical visualization of subcritical flow in a finite depth domain ($U_\infty/\sqrt{(gh)} = 0{\cdot}4$, where h is the undisturbed free stream depth); linear formulation

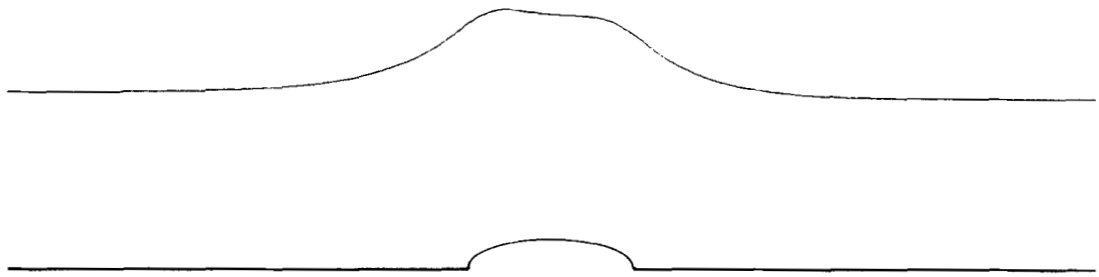

Figure 3. Free surface profile of supercritical flow in a finite depth domain ($U_\infty/\sqrt{(gh)} = 1{\cdot}2$); linear formulation

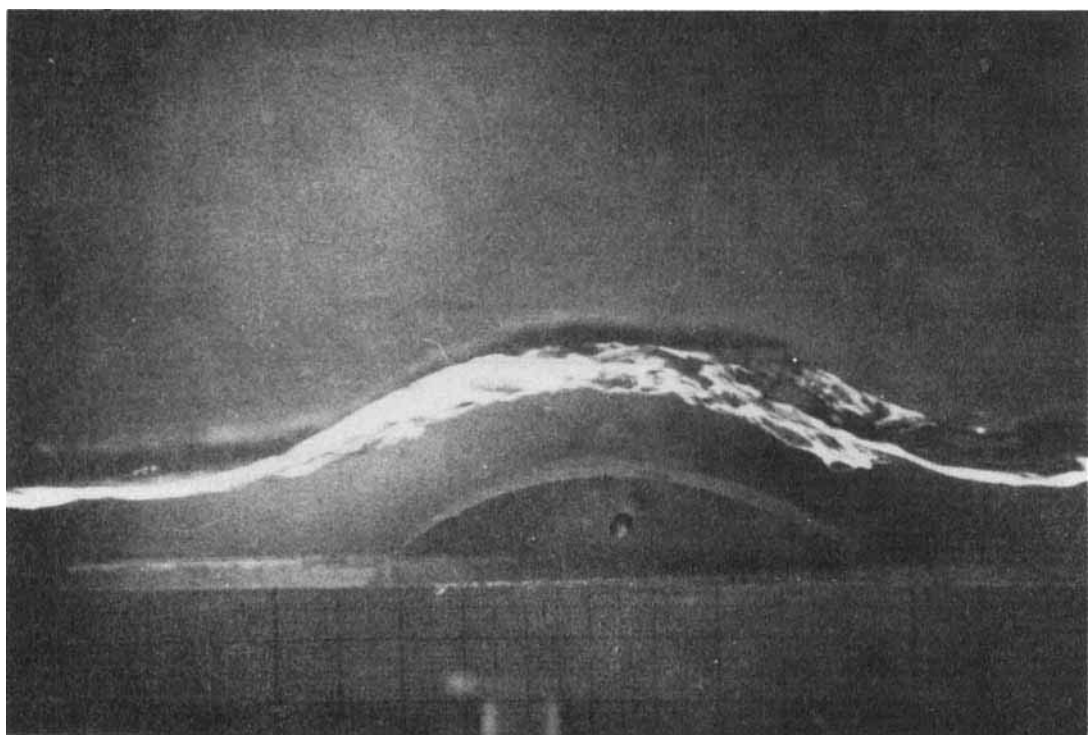

Figure 4. Supercritical flow ($U_\infty/\sqrt{(gh)}=2$). The free surface follows the shape of the obstacle without showing any downstream perturbation; the photograph is taken from Reference 15

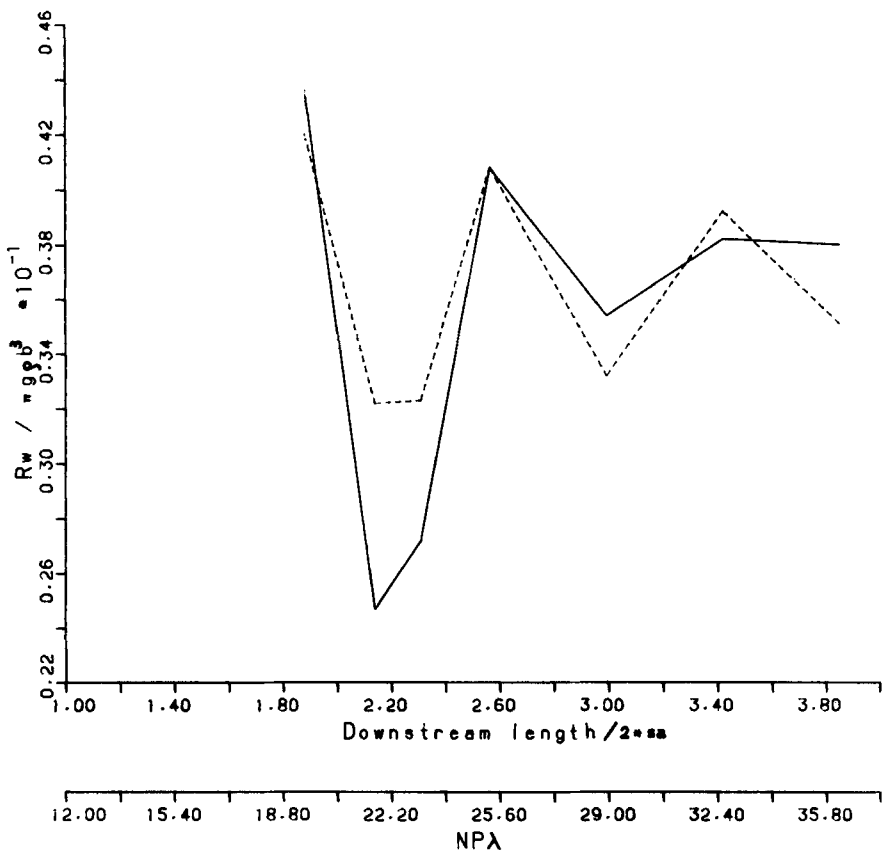

Figure 5. Computed wave resistance for a submerged sphere ($f/sa=2$, $Fr=U_\infty/\sqrt{(gf)}=0{\cdot}7$): - - - - - - - -, versus $NP\lambda$, with a fixed downstream extension of the panelled free surface, equal to 2·6;————, versus the downstream length, with $NP\lambda=24$

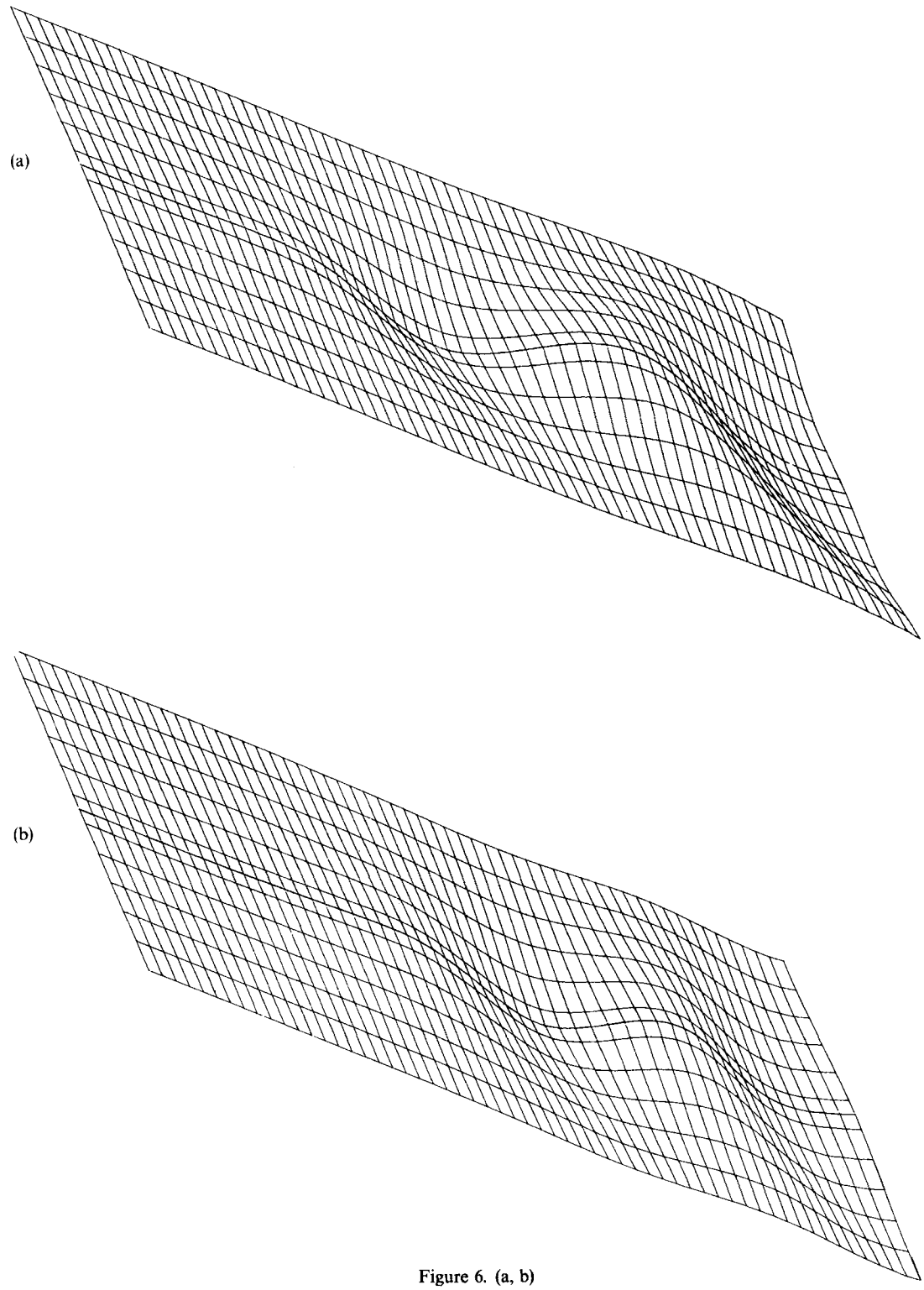

Figure 6. (a, b)

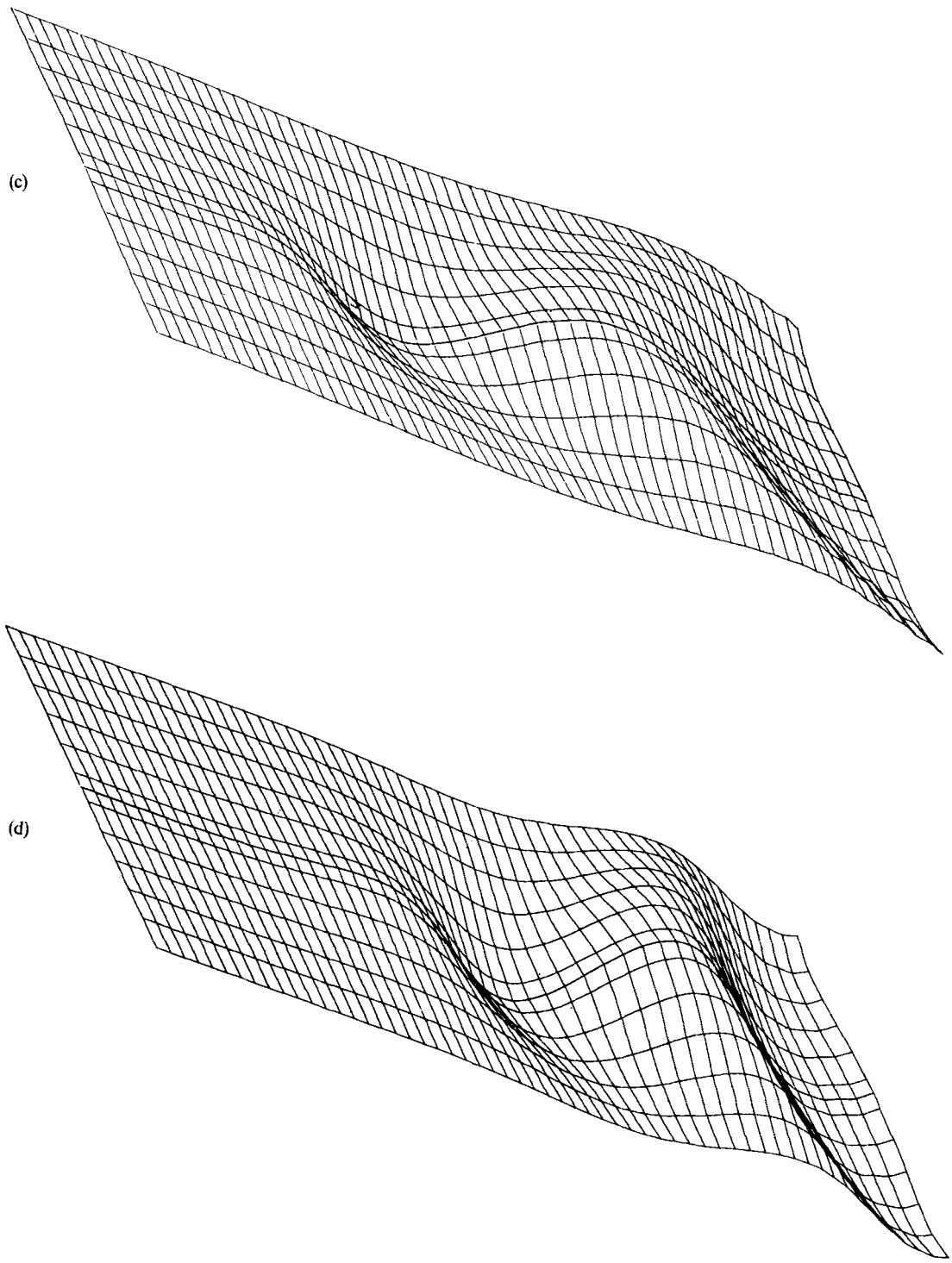

Figure 6. Three-dimensional wave pattern generated by a sphere and a prolate spheroid ($e = 0{\cdot}9165$) submerged in deep water ($f/sb = 2{\cdot}0$, $Fr = U_\infty/\sqrt{(gf)}$): (a) sphere, $Fr = 0{\cdot}60$; (b) spheroid, $Fr = 0{\cdot}60$; (c) sphere, $Fr = 0{\cdot}75$; (d) spheroid, $Fr = 0{\cdot}75$

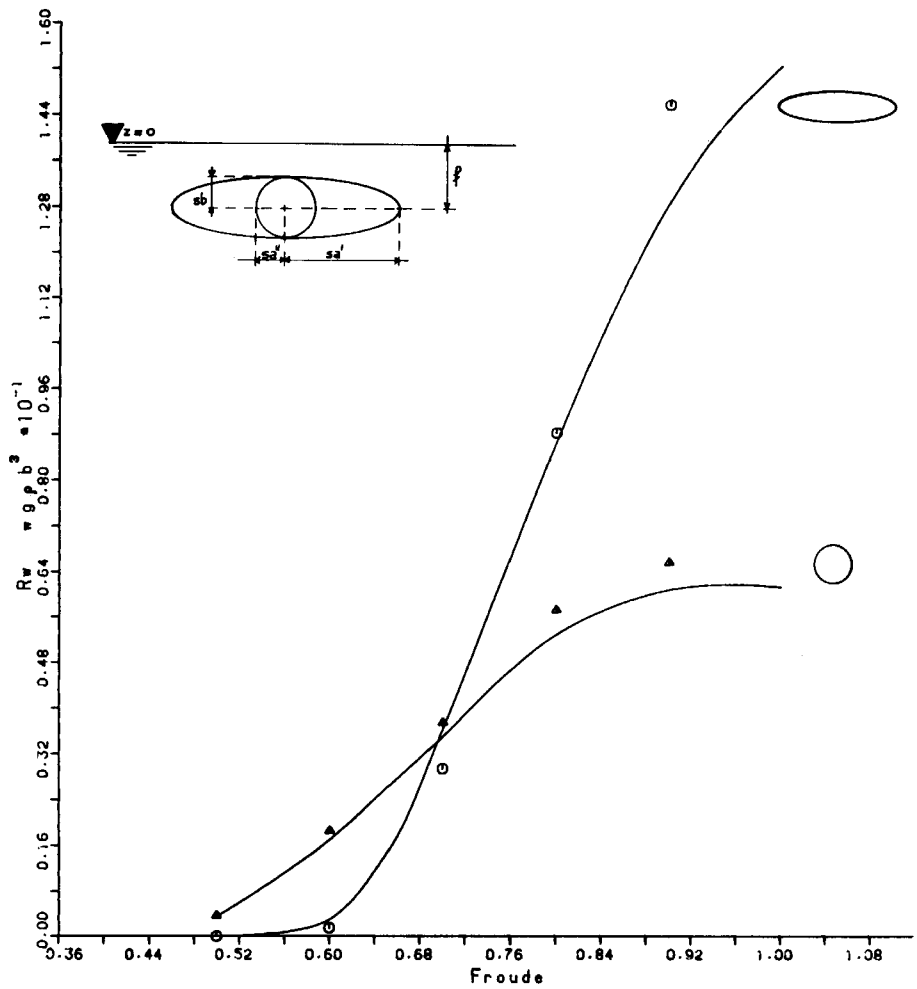

Figure 7. Wave resistance for submerged bodies as a function of the Froude number ($Fr = U_\infty/\sqrt{(gf)}$, $sa'/sa'' = 5/2$); ————, Havelock (analytical);[16] ⓘ, linear method for the prolate spheroid; ▲, linear method for the sphere

comparison is made between the analytical solution obtained in Reference 16 and the numerical results computed with the present linear method for the wave resistance of the same bodies.

ACKNOWLEDGEMENT

We wish to express our gratitude to Renzo Piva of the Department of Applied Mechanics, University of Rome, for his encouragement and useful suggestions for the development of this work.

REFERENCES

1. J. Wehausen, 'The wave resistance of ships', *Adv. Appl. Mech.*, **13**, 93–245 (1973).
2. Lord Kelvin, *Math. and Phys. Papers*, Cambridge, 1910.
3. N. E. Zhukovskii, 'On the wave of translation', *Complete Works, Vol. 4*, ONTI, 1937.

4. A. Tikhonov, 'Two-dimensional problem of the motion of a wing under the surface of a heavy fluid of finite depth', *Proc. USSR Acad. Sci.*, OTN, No. 4 (1940).
5. A. A. Kostyukov, *Theory of Ship Waves and Wave Resistance*, ECI, Iowa, 1968.
6. J. Wehausen and E. Laitone, 'Surface waves', *Handb. Phys., Vol. 9*, Springer-Verlag, 1960.
7. J. H. Michell, 'The wave resistance of a ship', *Phil. Mag.* **45,** 106–123 (1898); also in *The Collected Mathematical Works of J. H. and A. G. M. Michell*, Noordhoff, Groningen, 1964.
8. G. Gadd and N. Hogben, 'The determination of wave resistance from measurement of the wave pattern', *NPL, Ship Report 70,* 1965.
9. K. Eggers, S. Sharma and L. Ward, 'An assessment of some experimental methods for determining the wave making characteristics of a ship form', *Trans. SNAME* **75,** 112–157, (1967).
10. J. N. Newman, *Marine Hydrodynamics*, MIT Press, 1978.
11. C. W. Dawson, 'A practical computer method for solving ship-wave problems', *Second Int. Conf. on Numerical Ship Hydrodynamics*, Berkeley, 30–38, (1977).
12. H. Maruo and S. Ogiwara, 'A method of computation for steady ship-waves with non-linear free surface conditions', *Fourth. Int. Conf. Numerical Ship Hydrodynamics*, Washington, 1985, 218–233.
13. O. Daube and A. Dulieu, 'A numerical approach of the nonlinear wave resistance problem', *Third Int. Conf. on Numerical Ship Hydrodynamics*, Paris, 73–80, (1981).
14. C. Do and P. Guevel, 'Waves on a uniform flow in a channel of constant depth', in A. Fasano and M. Primicerio, Pitman Adv. Publ. Progr., Boston, *Free boundary problem: theory and applications, Research Notes in Mathematics*, 1983.
15. J. Cahouet, 'Etude numerique et experimentale du probleme bidimensionnel de la resistance de vagues non-lineaire', *Rapport de Recherche 185,* 1984.
16. T. H. Havelock, 'The wave resistance of a spheroid', *Proc. R. Soc. A,* **131,** 275–285 (1931).
17. E. Campana, F. Lalli, V. Bulgarelli,'A numerical solution of the nonlinear wave resistance problem for simple shaped submerged bodies', *Meccanica*, to be published.